Available online at www.sciencedirect.com
SCIENCE DIRECT®
Polymer 44 (2003) 5771–5777
polymer
www.elsevier.com/locate/polymer

DSC and DMTA study of annealed cold-drawn PET: a three phase model interpretation

A. Bartolotta, G. Di Marco, F. Farsaci, M. Lanza, M. Pieruccini*

CNR, Istituto per i Processi Chimico-Fisici Sez. Messina, Via La Farina 237, I-98123 Messina, Italy

Received 21 March 2003; received in revised form 2 May 2003; accepted 30 June 2003

Abstract

Cold-drawn poly(ethylene terephthalate) (PET) samples annealed at different undercoolings are studied by means of differential scanning calorimetry and dynamic mechanical thermal analysis. When heating from room temperature, the onset of the glass transition region in cold-drawn, un-annealed samples is found to be significantly lower than in the case of un-oriented PET. On the contrary, the presence of crystalline lamellae in oriented PET cause a shift (and spread out) of the glass transition region towards higher temperatures. The crystal thickening process caused by heating above the annealing temperature, is suggested to take place after a rigid amorphous phase linked to the basal surface of the lamellae has softened. It is found that the low-temperature (between 100 and 140 °C) annealed samples have a glass dispersion region ranging significantly above the annealing temperature itself. This circumstance leads to envisage vitrification as a possible mechanism able to limit lamellar thickening during the annealing process at these low temperatures.

Keywords: Poly(ethylene terephthalate); Drawing; Thermal-mechanical analysis

1. Introduction

The peculiar physical–chemical properties of poly(ethylene terephthalate) (PET) are subject of extensive investigation not only in view of the industrial applications of this material, but also for the wealth of interesting phenomenologies relating it to basic aspects of polymer physics in general.

This paper focuses on some observation concerning the mechanical and thermal behaviour of annealed cold-drawn PET samples, and is aimed at suggesting possible underlying mechanisms.

Differential scanning calorimetry (DSC) and dynamic mechanical thermal analysis (DMTA) on both un-oriented and cold-drawn, un-annealed PET have been reported in Ref. [1]. In that paper, the effect of a step-by-step annealing of oriented PET at subsequently increasing temperatures was also studied by wide angle X-ray scattering (WAXS) in order to investigate the evolution of crystalline structures.

On the other hand, the internal nano-structure of cold-drawn PET can be controlled by setting crystallinity and lamellar thickness through appropriate annealing procedures [2]. On this basis, a very interesting and stimulating systematic study of the relationship between the internal phase structure and the mechanical features (such as hardness, creep behaviour and Young modulus) of these PET samples, has been done by Asano et al. [2] and Flores et al. [3]. The micro-indentation technique used by these authors intrinsically probes long time scale modes, which are associated to long range chain motions.

In this scenario, wondering whether or not probing higher frequency modes in a DMTA setup is able to further improve our knowledge about the interplay of amorphous and crystalline phases in this kind of samples, deserves consideration.

The procedure we followed in preparing the samples was similar to that of Asano et al. [2], and is explicitly reported in Section 2. The DSC and DMTA results on the analyzed samples are reported in Section 3, and the effect of changing the annealing temperature is also commented on briefly, whenever the discussion can be kept clear of too much speculative digressions. At this stage, however, we found it useful to consider our observations in the light of a three phase model (where a further rigid amorphous phase is

* Corresponding author. Tel.: +39-090-2939528; fax: +39-090-2939902.
E-mail address: pieruccini@me.cnr.it (M. Pieruccini).

0032-3861/03/$ - see front matter © 2003 Elsevier Ltd. All rights reserved.
doi:10.1016/S0032-3861(03)00589-5

assumed to be present in the semicrystalline PET) in terms of which also Kattan et al. [4] discussed very recently their DSC and thermally stimulated depolarization currents results. Section 4 is devoted to a more speculative discussion, with the aim of giving a tentative description able to fit the relevant aspects of our observations. In doing this, we found the need to refer to the very important small angle X-ray scattering (SAXS) analyses by Imai et al. [5] and Asano et al. [2], because we think our picture finds support in the results presented by these authors.

2. Experimental

Fully amorphous PET films were furnished by Good-Fellow (ES 301465) in the form of foils with a thickness of 350 μm. Uniaxial oriented samples were obtained by drawing strips of PET, at room temperature, in a tester machine LR10K by LLOYD Instruments, using a tensile geometry. The strips were subjected to a drawing rate of 2 mm/min, and by neck propagation a natural draw ratio of ~4 was reached for all specimens. The final thickness was ~150 μm. Cold-drawn PET was afterwards annealed for 3 h in controlled atmosphere at different temperatures T_a [2,3]. Both the ends of the oriented films were tightened in a stainless steel clamp to avoid contraction along the drawing direction. The annealing temperatures were set with an accuracy of 0.1 °C in the interval 60 °C ≤ T_a ≤ 220 °C.

Mechanical properties of cold-drawn films (loss tangent and dynamical storage modulus, tan δ and E' respectively) were measured in the 25–200 °C temperature range by a dynamical mechanical thermal analyser of Polymer Laboratories (MKII). Dynamical experiments were carried out by using a bending geometry in a single cantilever configuration. The oriented samples were clamped so to probe the response associated to the bending of the average chain direction. The temperature scan rate was fixed at 2 °C/min with an accuracy of 0.1 °C and the frequencies were set to 0.3 and 3 Hz for all samples.

Calorimetric measurements were performed by Perkin–Elmer Pyris 1 differential scanning calorimeter, calibrated with Indium and Zinc standards. Thermograms were collected under a constant flux of nitrogen at 0.11 dm^3/min using typically 4–5 mg of samples with a heating rate of 40 °C/min in the 30–300 °C temperature interval. All DSC curves were baseline subtracted and normalized to 1 mg of sample.

3. Results

WAXS did not reveal significant traces of crystallinity neither in the un-oriented nor in the cold-drawn samples before any thermal treatment.

The DSC thermogram of the *un-oriented* un-annealed PET is reported in Fig. 1. Upon increasing the temperature

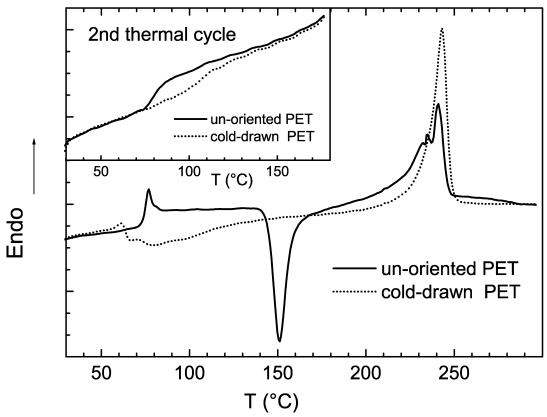

Fig. 1. DSC thermograms of un-oriented (continuous line) and cold-drawn (dotted line) PET samples, both un-annealed. In an expanded heat flux scale, but with a T-scale exactly matching the main frame of the figure, the inset shows the thermograms of similar samples after a heating cycle up to 180 °C and then cooled back to room temperature.

T, the glass transition region is crossed first, with an onset at $(T_g)_{onset} \approx 70$ °C. The transition ends at about 85 °C, and a crystallization peak is then observed, with an onset at $T \simeq 140$ °C. A rather wide and structured peak, associated to the multiple melting behaviour typical of PET and extensively studied calorimetrically by Kong et al. [6], then follows the crystallisation process. The value $T \simeq 285$ °C is the limit above which melting is not observable anymore.

For easy comparison with the case above, the thermogram of the *cold-drawn* un-annealed PET is reported in the same main frame of Fig. 1. Starting from 30 °C, the onset of the first endothermal process is now observed at a temperature lower by about 15 °C with respect to the un-oriented PET. This first increase of the heat capacity is ascribed to the onset of the glass transition (see also the discussion of the DMTA Fig. 2b below). In the light of

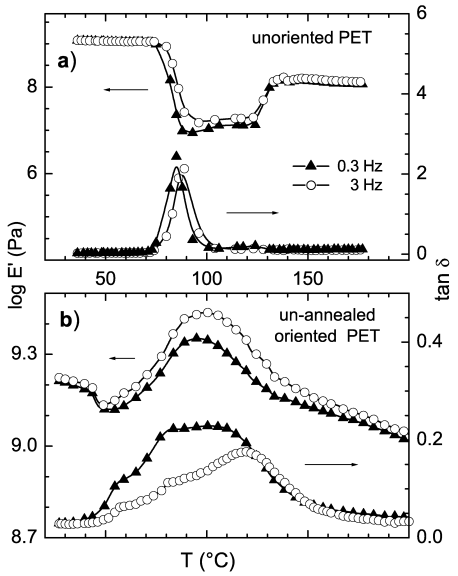

Fig. 2. Storage modulus E' and tan δ at 0.3 and 3 Hz for un-oriented (a) and oriented (b) PET samples, both un-annealed.

current ideas in polymer glasses [7], the observed change of $(T_g)_{onset}$ is somewhat unexpected, since both chain orientation and the expected density increase accompanying PET cold-drawing (see Ref. [2]) would suggest an opposite behaviour. It is possible that the further "anisotropic" internal stress imposed to an already out-of-equilibrium frozen system, inherent to forcing chain orientation in a glass (cold-drawing), may play a role in this "anomaly".

Differently from the un-oriented case, the glass transition onset is now suddenly followed by a transition to a different thermodynamic state, with an exothermal peak at $T \simeq 65$ °C. Then a rather widely spread-out process is observed, with a first peak at $T \simeq 80$ °C. As the temperature further increases, a still rather broad endothermal peak is found, but the upper limit for observable melting is now at $T \simeq 260$ °C.

The calorimetric analysis has also been carried out on un-oriented and cold-drawn samples which previously underwent a heating cycle up to a temperature of 180 °C (i.e. up to the end of the crystallisation process, just before the beginning of the multiple melting process), and were then cooled to room temperature before the DSC run. The resulting thermograms are reported in the inset of Fig. 1. In the case of the un-oriented sample the whole range of the glass transition is now shifted upwards by about 5 °C with respect to the case where no significant crystallinity is initially present (main frame of the figure). Of course, no crystallisation peak is observed before the melting region is reached.

The effect of the heating cycle is more dramatic in the case of the cold-drawn sample, which now shows a rather widely spread-out glass transition region in the interval 90 °C $< T <$ 130 °C, that is, with an onset considerably upwards shifted with respect to the case where no previous thermal cycle was imposed (main frame of the figure). Note that setting the upper temperature of the heating cycle below the melting onset prevents significant orientational relaxation of the chains.

From DMTA on the un-oriented sample, an activated dispersion region corresponding to the glass relaxation can be observed around $T \simeq 80$ °C (see Fig. 2a), followed by a slight pre-crystallisation stiffening. The latter can be possibly related to the density modulation preceding the formation of a crystalline phase, which was already observed by Imai et al. [5]: a pre-transition phenomenon more recently settled within the framework of the spinodal assisted crystallisation mechanism described by Olmsted et al. [8]. The rather steep increase of the elastic modulus observed in the range 125 °C $\leq T \leq$ 135 °C must be ascribed to the growth of crystalline domains (remind the relatively fast heating rate in DMTA to be compared with the large induction times in un-oriented PET [5]; on the other hand with reference to the crystallisation onset observable by DSC in Fig. 1, consider the much larger heating rate of 40 °C/min set for the latter technique).

Fig. 2b shows the mechanical behaviour of the oriented un-annealed sample. (Note that during DMTA the sample ends are clamped at a fixed distance, so that the contraction along the drawing direction is prevented much as like in the annealing procedure.) Upon increasing the temperature, starting from about 25 °C, the real part of the elastic modulus, E', decreases slightly until the value $T \simeq 45$ °C is reached, where this tendency is suddenly enhanced, since the glass dispersion region is being approached. The corresponding behaviour of tan δ clearly reveals the character of this process as a frequency dependent one. The elastic modulus then starts to increase upon further increasing of T, while tan δ reveals two non-activated (i.e. frequency independent) processes at $T \simeq 55$ °C and $\simeq 80$ °C. Recall that the SAXS analysis by Asano et al. [2] on cold drawn annealed samples similar to ours, did not reveal appreciable presence of triclinic structures after annealing at $T_a \leq 70$ °C, while only a weak appearance of the crystalline phase was found in samples annealed at $T_a =$ 80 °C. On the other hand, it is worth noticing that the sample starts stiffening already from ~55 °C (E' in Fig. 2b), i.e. in the temperature region where Asano et al. [2] have shown that smectic domains begin to form.

As the temperature further increases, the observed behaviour of the real part of the elastic modulus results from the mixed contributions of crystallisation and softening of the interlamellar regions.

The thermograms of the oriented samples annealed at different T_a's are reported in Fig. 3a and b. For a better representation, the endothermal melting peaks of the 160 °C $\leq T_a \leq$ 220 °C samples are plotted separately in Fig. 3b; the others look very similar to that of the $T_a = 160$ °C sample and are not reported.

Neither of the samples annealed at 65 and 75 °C (which are known not to reach significant crystallinity [2], if any) show crystallisation below 80 °C, even if during DSC analysis no external constraint is imposed to prevent sample contraction along the drawing direction (remind Fig. 1 for un-annealed cold-drawn PET). This means that an internal constraint develops anyway during the previous annealing

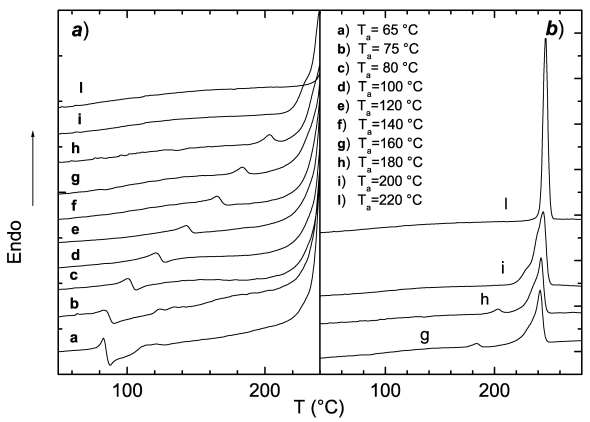

Fig. 3. DSC thermograms of oriented PET samples annealed at different T_a's. For a clear representation, part (a) reports the temperature interval up to the beginning of the melting region; part (b) shows some representative thermograms in an extended T-range.

at these low T_a's, which cannot be associated to crystallisation. In fact, the smectic domains forming at these temperatures [2] may well play a role as internal constraint. For both these low-T_a samples, crystallisation starts at the same $T \simeq 83$ °C, always preceded by a more or less pronounced endothermal process with an onset slightly above 70 °C.

Apart of the 65 and 75 °C annealed samples, almost all the other thermograms reported in Fig. 3 show an endothermal process located at a temperature T_r which is related to the annealing temperature by the approximate relationship $T_r = T_a + 20$ °C (for the $T_a = 220$ °C sample the T_r process, if existing, merges into the overall melting peak). A similar behaviour was found by Kong et al. [6], with almost the same constant $T_r - T_a$, on un-oriented PET crystallised at different temperatures.

For $T_a \leq 140$ °C a more or less pronounced exothermal contribution is visible just above T_r. For the samples annealed at $T_a < 80$ °C the latter must be associated with the first, significant, appearance of crystalline domains.

In the case of $T_a = 200$ °C the T_r process is still visible as a shoulder on the melting peak, whereas for $T_a = 220$ °C only a single endothermal process is observed, centered at about 245 °C, which however is much narrower than in other cases. This latter behaviour and the above relationship between T_a and T_r when a crystalline phase is present, appears as an hysteresis effect associated to lamellar melting, conforming to first order phase transitions [9].

Consider now the DMTA data. Most interesting are the results reported in Fig. 4, concerning the $T_a = 60$ °C sample. The elastic modulus E' reveals a slow stiffening process starting from about 40 °C, followed by a maximum around 70 °C and a remarkable (non-activated) dip at 80 °C. At the latter temperature crystallisation begins (cf. [2]) and the elastic modulus increases rapidly again. Then the process evolves as a superposition of both crystallisation and amorphous relaxation. When the sample temperature rises above 40 °C, further formation of smectic domains together with some enhancement in rearrangement processes occurring either into the already existing smectic domains (perfectioning), or in their peripheral regions, may take place. These would contribute to the observed slight increase in E'. The subsequent activated rapid E' decrease in the interval 70 °C $< T <$ 80 °C (with regard to the lower bound, compare also the "a" and "b" thermograms in Fig. 3a, in both of which the onset of the first endothermal process is observable within the same temperature interval) is difficult to interpret in detail, because it may result from a convolution of a number of processes, among which the softening of rigid non-crystalline and/or glassy domains would be of relevance as precursors to the formation of crystalline regions. In fact however, the rather high sensitivity of the mechanical response to the excitation frequency in this region is indicative of the major role played by those rearrangement modes typically involved in the glass transition process. Note that the crystallisation process starts rapidly right above the $T = 80$ °C threshold. This of course can be attributed to the fact that in the present case the chains are pre-oriented, since rather long induction periods (~120 min) for crystal formation are reported by Imai et al. [5] for un-oriented PET annealed at $T_a = 80$ °C.

Fig. 5 collects the DMTA data concerning representative samples annealed at $T_a \geq 100$ °C. Fig. 6, on the other hand, shows that DSC and DMTA at 0.3 Hz can be substantially superimposed with regards to glass transition region and endothermal process at T_r. From the E' vs. T dependencies of Fig. 5, the frequency independent processes at T_r already observed in the corresponding DSC thermograms are easily

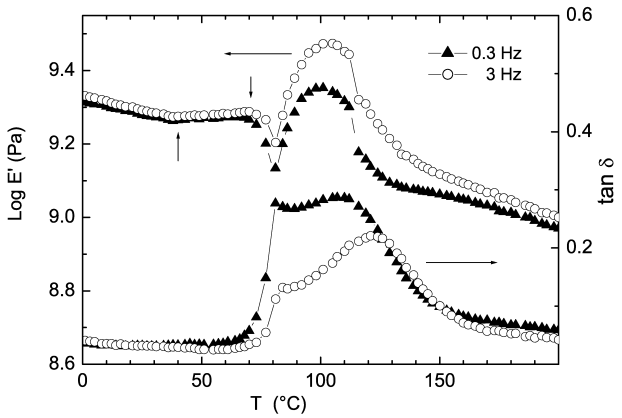

Fig. 4. Storage modulus E' and tan δ at 0.3 and 3 Hz for the $T_a = 60$ °C annealed oriented sample, where the crystalline phase is not initially present.

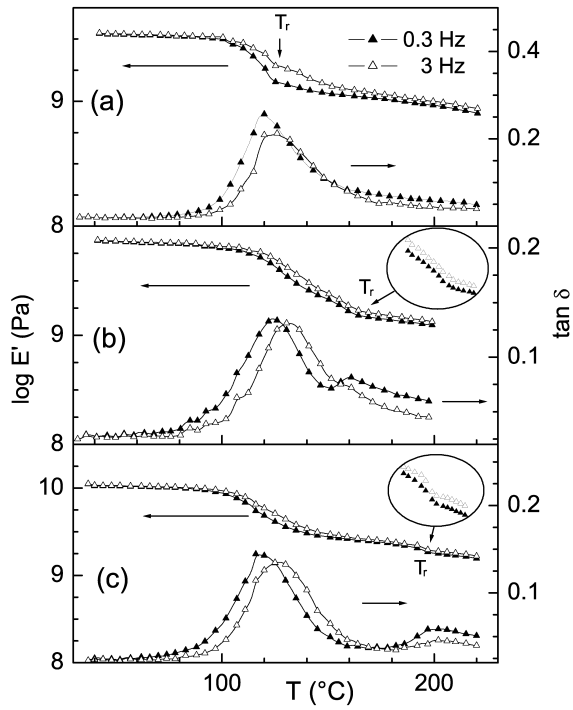

Fig. 5. Storage moduli E' and tanδ' s at 0.3 and 3 Hz for representative samples annealed at 100 °C (a), 140 °C (b) and 180 °C (c). Note the decrease in d(Log E')/dT before T_r is approached from below (the relevant regions are duly expanded for the sections b and c of the figure).

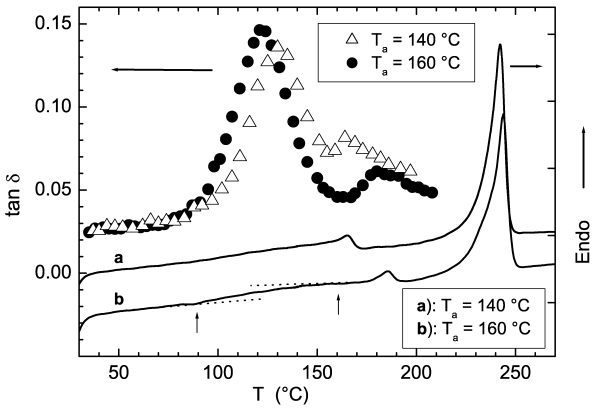

Fig. 6. Comparison between tan δ at 0.3 Hz and DSC results for the samples annealed at $T_a = 140$ and 160 °C. Note that the superposition of the glass dispersion and the T_r process is still present at $T_a = 140$ °C but is substantially absent at $T_a = 160$ °C.

identified. It is important to note that an appreciable decrease of the modulus always precedes these transitions. The subsequent discontinuous decrease of the slope d(Log E')/dT suggests that a comparatively fast further crystallisation process is being observed above T_r.

Concerning the tan δ vs. T data, the $T_a = 100$ °C sample is characterized by just one dispersion region, the maximum value of which is rather larger than in other cases. The corresponding E' behaviour, however, reveals that the loss peak consists of both the contributions of the glass relaxation and the process at T_r. For higher values of T_a, the two contributions are more clearly separated, with the glass dispersion region shifting towards higher temperatures upon increasing the excitation frequency, while the dispersion around T_r remaining fixed. It is worth noticing that the relationship $T_r \simeq T_a + 20$ °C holds *independent* of whether T_r falls within the glass transition range or not. This suggests that the process associated to T_r may occur within non-glassy domains embedded in the oriented glass.

4. Discussion and concluding remarks

As a first point to comment about, we draw attention onto the dependence of $(T_g)_{onset}$ on the presence and the nature of the structural heterogeneities characterising cold-drawn samples with different thermal history. To this aim, DMTA results suffice as a reference (Figs. 2, 4 and 5). Un-annealed cold-drawn PET, which is characterised by only gross chain orientational order, shows the lowest value of the glass transition onset, i.e. $(T_g)_{onset} \sim 40$ °C (Fig. 2b; see also the related comment to Fig. 1 at the beginning of the previous section). On the other hand the presence of crystalline domains, i.e. regions of comparatively highest structural order and density, shifts $(T_g)_{onset}$ up to ~90 °C independent of T_a (Fig. 5).

In the case where only smectic domains are present ($T_a =$ 60 °C), we can estimate $(T_g)_{onset} \sim 70$ °C from the steep (activated) softening observable right below the $T = 80$ °C threshold in Fig. 4. So, the latter (intermediate) value of $(T_g)_{onset}$ is found in the presence of structures of intermediate order between the crystal and the (homogeneous) oriented glass.

Apart from the peculiarities of the un-annealed cold-drawn sample, free volume concepts would fit the $(T_g)_{onset}$ upwards shifting, if an increase of the average density of the glassy domains goes together with the appearance of structures of increasing order and density. In the light of this observation, chain stiffness and connectivity assume a central role in linking the properties of the bulk glass to those of the ordered structures possibly present.

We now turn to consider our DMTA and DSC results with regard to the process observed at a temperature T_r varying with the annealing temperature, when the crystalline phase is present. We restrict our discussion to the samples annealed at $T_a \geq 100$ °C, where besides crystalline regions, further significant presence of smectic domains can be safely excluded [2]. In this context, we propose an interpretation of our results in terms of just a three phase model, where apart of ordinary amorphous bulk, rigid non-crystalline domains accompanying the presence of the crystalline phase in PET are also accounted for.

From DMTA we first observe that the onset of the glass dispersion region, i.e. when the activation of the less constrained vibrational modes starts taking place, is substantially independent of T_a (Fig. 5). The early de-freezing of glassy regions which are far enough apart of the crystallites would be consistent with this observation. Besides, the difference $T_r - T_a \simeq$ const., which shows up as a threshold to be overcome for a significant crystallisation rate to be observed, is independent of where T_a (or T_r) is located with respect to the glass dispersion region. In particular, this phenomenology is found to characterise the samples with $T_a \geq 160$ °C, i.e. when no glassy regions should be present anymore. The strict regularity of the $T_r \equiv T_r(T_a)$ dependence suggests, in analogy with the idea underlying the relationship between lamellar thickness l and undercooling (i.e. $l \propto \sigma_e/|\mu_c - \mu_a|$, with σ_e the basal surface tension and $\mu_{c/a}$ the chemical potential of a monomer in the crystalline/amorphous phase), that it may come about as a result of an interplay between the crystalline bulk and adjoining non-crystalline domains in the basal regions of the lamellae.

With this picture in mind, the crystallisation process associated to T_r then would consist of a lamellar thickening. Considering now the whole set of samples with $T_a \geq 100$ °C, we suggest that the thickening process may well take place, always within isolated non-glassy regions (remind the case with $T_a = 100$ °C, where the annealing temperature is at the lower bound of the glass dispersion region at 0.3 Hz, and still the relationship $T_r \simeq T_a + 20$ °C holds).

Concerning DMTA and DSC we observe that all samples share the common feature that (much like in the case of the $T_a = 60$ °C sample, just below $T_a = 80$ °C) the elastic

modulus undergoes a fast decrease right before each T_r is approached from below, a process always accompanied by an increase of the specific heat.

In our picture we ascribe all this to the softening of rigid non-crystalline regions adjoining the basal lamellar planes, as a precursor to lamellar thickening. In this scenario, the impressive narrowing of the melting peak (the latter consisting of a sequence of melting/recrystallisation processes) for the $T_a = 220$ °C sample (Fig. 3b), finds an easy interpretation.

The idea of resorting to the hypothesis of a rigid amorphous phase in order to interpret the peculiar behaviour of semi-rigid polymers is not new [10,11], but is increasingly being considered for the interpretation of the experimental data [4,12–14]. This concept, however, is also subjected to some criticism [15]. One major doubt rises from the observation that if two kinds of amorphous phases exist, then one should expect to observe two glass transition regions. We point out, however, that this conclusion may not be justified in the case, for instance, where the two amorphous regions merge one into each other through a diffuse interface. And in fact, we observe that the glass transition region spreads out towards higher temperatures as an effect of crystal formation (Fig. 1). When going from the amorphous bulk towards the basal lamellar interfaces, the chain segments experience ever increasing constraints, which may well justify higher temperatures for the de-freezing of the vibrational modes. This picture fits well with the comments by Kattan et al. [4] (end of section 3.2 of that paper), who ascribe the spread-out of the glass dispersion to some inhomogeneity of the glass itself.

One further important implication follows from this picture. Our DMTA results show that the glass dispersion ranges almost invariably in the 90 °C $< T <$ 160 °C interval for all considered $T_a \geq 100$ °C, and that the process at T_r (function of T_a) falls within this range unless $T_a > 140$ °C. Consider now the 100 °C $\leq T_a \leq$ 140 °C samples, for which we are led to adopt the picture of semi-crystalline domains embedded in a glass. During the annealing procedure, the formation of rigid amorphous regions (or internal constraints in general) is inherent to crystallisation; so, it may be possible that lamellar thickening is limited by a rubber-to-glass transition taking place, at constant temperature, within the interlamellar regions *during* crystal formation. This is because these semi-crystalline regions are regularly distributed to form stacks allowing for a long period to be measured [2]. Moreover, if the glass transition would not intervene, the forming lamellae would reach larger thicknesses.

This idea finds support from the SAXS data of Asano et al. [2], which for easy reference are reported in Fig. 7 in the form of a Gibbs–Thomson plot (note the presence of the extra point obtained by Asano et al. for $T_a = 240$ °C, an annealing temperature not considered in our present analysis). The data obtained by Imai et al. [5] from un-oriented PET are also shown in the same figure. A linear fit

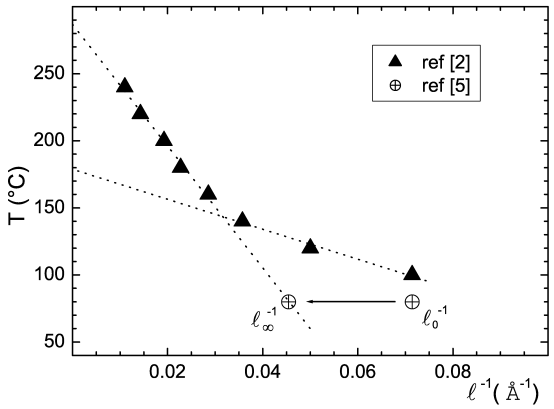

Fig. 7. Gibbs–Thomson plot [T vs. l^{-1} Å^{-1}] of the data from Asano et al. [2] and from Imai et al. [5]. The dotted lines are best fits extrapolating to (apparent) ideal equilibrium melting points.

to the $T_a \geq 160$ °C data of oriented PET extrapolates to an equilibrium melting point $T_m^\infty \simeq 285$ °C (including $T_a =$ 140 °C in the fitting procedure would lead to $T_m^\infty \simeq 280$ °C). On the other hand, the linear fit to the $T_a \leq 140$ °C data lead to a much lower value of T_m^∞. The lamellae grown at lower annealing temperatures are thus thinner than if the Gibbs–Thomson relation would hold in the whole explored range of annealing temperatures. We now observe that the lamellar thickness measured by Imai et al. [5] in un-oriented PET annealed at $T_a = 80$ °C is initially $l_0 = 14$ Å. Then, after an annealing time at the same T_a of ~60 min, the lamellar thickness levels off to a value $l_\infty = 22$ Å, i.e. very close to the extrapolation to low T_a's of the fit to Asano data. On the other hand, the crystal formation in oriented PET is characterised by induction times considerably shorter than in the case of un-oriented PET, while the measurements performed in [2] have been carried out after annealing times of order 180 min, and still the lamellar thickness is found to remain small. Remind, as a further quick reference to calorimetric results, that the thermograms shown in the inset of Fig. 1 report a rather significant upward shift and spreading out of the glass transition region in the oriented samples, if compared to the un-oriented ones, as an effect of the presence of crystalline lamellae.

In the light of our DMTA and DSC results, the above discussion of the SAXS data available in the literature give support to the idea of vitrification as a crystallisation induced process possibly opposing lamellar thickening in (low temperature annealing) oriented PET.

In a different context, Schick et al. [16] also envisaged similar mechanisms in order to discuss their temperature modulated DSC results from different *un-oriented* polymeric species. This represents an important independent support to the idea outlined above.

In conclusion, we found convenient to discuss our results by resorting to the hypothesis that rigid non-crystalline regions exist in the analyzed oriented samples. Although a quantitative characterisation of these regions is not given, some indirect evidence of their effectiveness has been

pointed out. The proposed hypothesis of a crystallisation induced rubber-to-glass transition, has not to be considered a firm conclusion from our analysis, but rather to be a stimulus for further investigations in this interesting field.

Acknowledgements

The authors wish to thank Dr A. Visco of the Department of Materials Engineering of the University of Messina for the help to prepare the cold-drawn PET samples.

References

[1] Göschel U. Polymer 1996;37:4049.
[2] Asano T, Calleja FJB, Flores CA, Tanigaki M, Mina MF, Sawatari C, Itagaki H, Takahashi H, Hatta I. Polymer 1999;40:6475.
[3] Flores A, Calleja FJB, Asano T. J Appl Phys 2001;90:6006.
[4] Kattan M, Dargent E, Grenet J. Polymer 2002;43:1399.
[5] Imai M, Kaji K, Kanaya T. Macromolecules 1994;27:7103.
[6] Kong Y, Hay JN. Polymer 2003;44:623.
[7] Mc Kenna GB. In: Allen G, Bevington JC, editors. Glass formation and glassy behavior. Comprehensive polymer science, vol. 2. New York: Pergamon; 1989.
[8] Olmsted PD, Poon WCK, McLeish TCB, Terrill NJ, Ryan AJ. Phys Rev Lett 1998;81:373.
[9] Chaikin PM, Lubensky TC. Principles of condensed matter physics. Cambridge: Cambridge University Press; 1995.
[10] Huo P, Cebe P. J Polym Sci Polym Phys 1992;30:239.
[11] Mathot VBF. Thermal characterization of states of matter. In: Mathot VBF, editor. Calorimetry and thermal analysis of polymers. Munich: Hanser; 1994.
[12] Wübbenhorst M, de Rooji AL, van Turnhout J, Tacx J, Mathot V. Coll Polym Sci 2001;279:525.
[13] Gutiérrez MCG, Rueda DR, Calleja FJB, Stribeck N, Bayer RK. Polymer 2003;44:451.
[14] Wunderlich B. Prog Polym Sci 2003;28:383.
[15] Boyd RH, Liu F. Dielectric spectroscopy of semicrystalline polymers. In: Runt JP, Fitzgerald JJ, editors. Dielectric spectroscopy of polymeric materials. Washington, DC: American Chemical Society; 1997.
[16] Schick C, Wurm A, Mohammed A. In: Reiter G, Sommer J-U, editors. Polymer crystallization: observations, concepts and interpretations. Springer series Lecture Notes in Physics; 2003. Chapter 14.